C. R. Mecanique 341 (2013) 257–265

Contents lists available at SciVerse ScienceDirect

Comptes Rendus Mecanique

www.sciencedirect.com

Combustion, flow and spray dynamics for aerospace propulsion

Numerical investigation of a helicopter combustion chamber using LES and tabulated chemistry

Pierre Auzillon [a,b,*], Eléonore Riber [c], Laurent Y.M. Gicquel [c], Olivier Gicquel [a,b], Nasser Darabiha [a,b], Denis Veynante [a,b], Benoît Fiorina [a,b]

[a] CNRS, UPR 288, Laboratoire d'énergétique moléculaire et macroscopique, combustion (EM2C), grande voie des vignes, 92290 Châtenay-Malabry, France
[b] École centrale Paris, grande voie des vignes, 92290 Châtenay-Malabry, France
[c] CERFACS, CFD Team, 42, avenue G. Coriolis, 31057 Toulouse cedex 01, France

ARTICLE INFO

Article history:
Available online 11 January 2013

Keywords:
Turbulent combustion modeling
Large Eddy Simulation
Tabulated chemistry

ABSTRACT

This article presents Large Eddy Simulations (LES) of a realistic aeronautical combustor device: the chamber CTA1 designed by TURBOMECA. Under nominal operating conditions, experiments show hot spots observed on the combustor walls, in the vicinity of the injectors. These high temperature regions disappear when modifying the fuel stream equivalence ratio.

In order to account for detailed chemistry effects within LES, the numerical simulation uses the recently developed turbulent combustion model F-TACLES (Filtered TAbulated Chemistry for LES). The principle of this model is first to generate a lookup table where thermochemical variables are computed from a set of filtered laminar unstrained premixed flamelets. To model the interactions between the flame and the turbulence at the subgrid scale, a flame wrinkling analytical model is introduced and the Filtered Density Function (FDF) of the mixture fraction is modeled by a β function. Filtered thermochemical quantities are stored as a function of three coordinates: the filtered progress variable, the filtered mixture fraction and the mixture fraction subgrid scale variance. The chemical lookup table is then coupled with the LES using a mathematical formalism that ensures an accurate prediction of the flame dynamics. The numerical simulation of the CTA1 chamber with the F-TACLES turbulent combustion model reproduces fairly the temperature fields observed in experiments. In particular the influence of the fuel stream equivalence ratio on the flame position is well captured.

1. Introduction

Aircraft industry introduces new combustion chamber technologies to decrease fuel consumption and pollutant emissions. Combustion occurs mainly in a premixed-like regime in order to control the flame temperature and consequently the pollutant emissions such as nitrogen oxides [1]. However, as fuel and oxidizer remain injected separately in the combustion chamber, complex stratified flames are generally observed [2]. It is the case of the helicopter gaz turbine combustor CTA1, designed by TURBOMECA, where a fuel stream composed of both air and kerosene is injected in the combustion chamber. Additional air is introduced through secondary inlets and dilution holes generate fuel stratification. It has been

* Corresponding author at: CNRS, UPR 288, Laboratoire d'énergétique moléculaire et macroscopique, combustion (EM2C), grande voie des vignes, 92290 Châtenay-Malabry, France.

E-mail addresses: pierre.auzillon@ecp.fr (P. Auzillon), eleonore.riber@cerfacs.fr (E. Riber), Laurent.Gicquel@cerfacs.fr (L.Y.M. Gicquel), olivier.gicquel@ecp.fr (O. Gicquel), nasser.darabiha@ecp.fr (N. Darabiha), denis.veynante@ecp.fr (D. Veynante), benoit.fiorina@ecp.fr (B. Fiorina).

1631-0721/$ – see front matter
http://dx.doi.org/10.1016/j.crme.2012.10.021

experimentally observed that the wall surface temperature is strongly affected by the fuel stream equivalence ratio. Indeed, hot spots are observed under nominal conditions in the vicinity of the injector but disappear when the fuel stream equivalence ratio is increased. The lack of experimental data motivates a numerical investigation of this combustion chamber in order to explain why the wall surface temperature is sensitive to the fuel stream injection conditions.

High performances Large Eddy Simulations are nowadays sufficiently mature to permit the computation of real gas turbines combustors [3–5]. The numerical simulations remains however very challenging because of both importance of the unsteady phenomena and the complexity of the chemistry. Tabulated chemistry methods have been developed to introduce detailed chemistry effects in numerical simulations with affordable CPU cost. Various strategies based on mathematical analysis such as Intrinsic Low-Dimensional Manifold (ILDM) [6], or based on physical considerations like Flame Prolongation of ILDM (FPI) [7,8] and Flamelet Generated Manifold [9], have been suggested to construct lookup tables where thermochemical quantities are stored. Different solutions are then possible to introduce tabulated chemistry effects in LES. The FPI-PCM [10] method accounts for mixture fraction subgrid scale fluctuations with the introduction of a presumed β filtered density function for the mixture fraction. However this approach does not capture the correct propagation speed of the flame front as shown in [11]. As suggested by Kuenne et al. [12], the thickened flame model (TFLES) combined with tabulated chemistry is a possible strategy that captures the flame speed, but this approach does not account for the impact of mixture fraction subgrid scale fluctuations on the flame propagation speed. A recent technique called Filtered Tabulated Chemistry for LES (F-TACLES) [11,13] has been proposed to include detailed chemistry in LES. It consists in generating a chemical lookup database from filtered 1-D laminar unstrained premixed flames computed with detailed chemical schemes. This method has been developed to capture the correct flame propagation speed under practical LES grid conditions, i.e. when the subgrid scale flame wrinkling is either resolved or partially-resolved [11]. The extension of the model to partially-premixed regimes has been proposed by Auzillon et al. [13] with accounting for mixture fraction heterogeneities at the subgrid scale. Numerical studies show that F-TACLES also provides a good prediction of the flame dynamics [14].

The objective of this paper is to perform a numerical investigation of the CTA1 combustion chamber to understand the effect of the fuel stream equivalence ratio on the flame position. The F-TACLES model, used to perform the computation, is briefly described in the first section. Mathematical details and model validations are given in [11,13]. The second section is dedicated to the CTA1 simulations. After a description of the configuration, the construction of the kerosene/air thermochemical database is discussed. The simulations results are then presented. The impact of the fuel stream enrichment on the wall surface temperature is retrieved and a physical explanation is proposed.

2. F-TACLES for stratified flames

The FPI technique [7,8] is retained here to determine low-dimensional trajectories covered by combustion chemistry. The chemical subspace accessed by a stratified flame in a complex geometry configuration is mapped by a collection of 1-D laminar premixed flames computed for various equivalence ratio within the flammability limits using detailed chemistry. This assumption is relevant for premixed and partially premixed flames [15]. However, errors are introduced in non-premixed regions, when mass diffusion through iso-equivalence ratio surfaces dominates. Nevertheless, these errors are limited when the fuel feeding stream is close to the rich mixture flammability limits [15], as in the combustor investigated here (equivalence ratio of the fuel stream are either 4 or 6.7 whereas the rich flammability limit of kerosene/air is about 3.7 [16]). In addition to that, because of micro-mixing phenomena, turbulent non-premixed flames may be piloted by leading edge flames which exhibit a lean premixed flame region [17] well captured by FPI tabulation.

In the present study, laminar thermochemical quantities are stored in a lookup table as a function of two coordinates: the progress variable Y_c which evolves monotonically between fresh and burnt gases and a mixture fraction z equal to zero in pure oxidizer and unity in pure fuel. For methane–air combustion, preliminary studies have shown that an efficient definition of this progress variable is obtained from a linear combination of CO_2 and CO mass fractions: $Y_c = Y_{CO} + Y_{CO_2}$ [8]. Such a definition of Y_c ensures a one-to-one correspondence between species and the progress variable.

The methodology F-TACLES has been recently developed to include tabulated chemistry in LES of turbulent stratified flames [14]. For that purpose a filtered chemical lookup database is generated from the FPI database. One-dimensional laminar propagating flames are filtered using a Gaussian filter while the filtered density function of the mixture fraction is described by a β-function. Any filtered thermochemical quantity is then stored in a 4-D table $[\Delta, \widetilde{Y}_c, \widetilde{z}, \widetilde{z''^2}]$ where Δ is the filter width. $\widetilde{Y}_c$ and $\widetilde{z}$ are the Favre filtered value of the progress variable and mixture fraction, respectively and $\widetilde{z''^2}$ is the subgrid scale variance of the mixture fraction. A constant value of Δ that ensures a sufficient resolution of the filtered flame front is chosen in the present article. The closure schemes for $\widetilde{z}$ and $\widetilde{z''^2}$ balance equations are quite usual [18] and are not discussed here. The transport equation for $\widetilde{Y}_c$ reads:

$$\frac{\partial \bar{\rho}\widetilde{Y}_c}{\partial t} + \nabla\cdot(\bar{\rho}\widetilde{\mathbf{u}}\widetilde{Y}_c) = \nabla\cdot(\overline{\rho D \nabla Y_c}) - \nabla\cdot(\bar{\rho}\widetilde{\mathbf{u}Y_c} - \bar{\rho}\widetilde{\mathbf{u}}\widetilde{Y}_c) + \bar{\rho}\widetilde{\dot{\omega}}_{Y_c} \tag{1}$$

where ρ is the density, $\mathbf{u}$ the velocity vector, and D the diffusivity. $\dot{\omega}_{Y_c}$ is the progress variable reaction rate expressed in s^{-1}. The closures of the Right Hand Side (RHS) terms are briefly summarized bellow. A more extensive discussion is available in Ref. [14].

2.1. Filtered chemical reaction source term $\widetilde{\dot{\omega}}_{Y_c}$

The filtered reaction rate $\widetilde{\dot{\omega}}_{Y_c}$ is modeled as [14]:

$$\widetilde{\dot{\omega}}_{Y_c} = \frac{1}{\bar{\rho}} \Xi \int_0^1 \langle \rho \dot{\omega}_{Y_c} | z = z' \rangle P(z') \, \mathrm{d}z' \tag{2}$$

where Ξ is the subgrid scale flame wrinkling factor and $P(z')$ is the subgrid scale FDF of the mixture fraction. $\langle \rho \dot{\omega}_{Y_c} | z = z' \rangle$ is estimated by filtering a 1-D laminar premixed flamelet computed at a given mixture fraction z:

$$\langle \rho \dot{\omega}_{Y_c} | z = z' \rangle = \int_{-\infty}^{+\infty} \rho^* \dot{\omega}^*_{Y_c}(x'_n, z') G_\Delta(x_n - x'_n) \, \mathrm{d}x'_n \tag{3}$$

The * superscript denotes quantities issued from a 1-D laminar unstrained premixed flame computed in the direction normal to the flame front x_n for a constant equivalence ratio (or mixture fraction z). In this article, $P(z)$ is modeled by a β-function parametrized by the first and second order moments of the mixture fraction: $\widetilde{z}$ and $\widetilde{z''^2}$. The filtered reaction rate $\widetilde{\dot{\omega}}_{Y_c}$ is in practice pre-computed and stored in a four-dimensional lookup database, $\widetilde{\dot{\omega}}_{Y_c} = \widetilde{\dot{\omega}}^*_{Y_c}[\widetilde{Y}_c, \widetilde{z}, S_z, \Delta]$ where $S_z = \widetilde{z''^2}/(\widetilde{z}(1-\widetilde{z}))$ is the unmixedness factor.

2.2. Filtered laminar diffusion terms

The model for the filtered molecular diffusion reads:

$$\nabla \cdot (\overline{\rho D \nabla Y_c}) = \nabla \cdot (\alpha_{Y_c} \bar{\rho} \widetilde{D} \nabla \widetilde{Y}_c) \tag{4}$$

where the correction factor α_{Y_c} is estimated from 1-D filtered premixed flames:

$$\alpha_{Y_c}[\widetilde{Y}_c, \widetilde{z}, S_z, \Delta] = \frac{\overline{\rho^* D^* \frac{\partial Y^*_c}{\partial x_n}}}{\bar{\rho} \widetilde{D} \frac{\partial \widetilde{Y}^*_c}{\partial x_n}} \tag{5}$$

where the laminar diffusivity is computed assuming unity Lewis number $D^* = \lambda^*/\rho^* C^*_p$ and the filtered diffusivity $\widetilde{D}$ is pre-computed and stored in the filtered lookup table as explained in Ref. [14]. As for the progress variable reaction rate, $\alpha_{Y_c} = \alpha_{Y_c}[\widetilde{Y}_c, \widetilde{z}, S_z, \Delta]$ is stored in the lookup database.

2.3. Subgrid scale convection term

The unresolved convection terms are modeled as:

$$\nabla \cdot (\bar{\rho} \widetilde{\mathbf{u} Y_c} - \bar{\rho} \widetilde{\mathbf{u}} \widetilde{Y}_c) = \Xi \left(\overline{\rho_0(z) S_l(z) \frac{\partial Y^*_c}{\partial x_n}} - \overline{\rho_0(z) S_l(z)} \frac{\partial \widetilde{Y}^*_c}{\partial x_n} \right) + \nabla \cdot \left((\Xi - 1) \alpha_{Y_c} \bar{\rho} \widetilde{D} \nabla \widetilde{Y}_c \right) \tag{6}$$

$$= \Xi \Omega_{Y_c}[\widetilde{Y}_c, \widetilde{z}, S_z, \Delta] + \nabla \cdot \left((\Xi - 1) \alpha_{Y_c} \bar{\rho} \widetilde{D} \nabla \widetilde{Y}_c \right) \tag{7}$$

where the first RHS term corresponds to the thermal expansion, estimated from one-dimensional detailed chemistry laminar premixed flames and stored in a 4-D lookup database $\Omega_{Y_c}[\widetilde{Y}_c, \widetilde{z}, S_z, \Delta]$. The second RHS term models the unresolved transport due to turbulence through a usual gradient formulation. The F-TACLES approach described here is implemented in the compressible LES code AVBP [19] using the Tabulated Thermochemistry for Compressible flow (TTC) formalism [20].

3. Numerical study of the CTA1 combustion chamber

3.1. Operating conditions of the investigated cases

As mentioned in the introduction, the present work focuses on the helicopter gaz turbine combustor CTA1, designed by TURBOMECA. The combustion chamber geometry is shown in Fig. 1. In this device, liquid kerosene mixes with air and vaporizes when flowing through the injection pipes. Therefore, a gaseous and homogeneous fuel stream penetrates the combustion chamber. The fuel stream temperature at the injection pipe exit is 575 K. Additional streams of air are introduced through secondary inlets and dilution holes. Under nominal operating conditions, the combustion chamber pressure is equal to 5 bar and the fuel stream equivalence ratio ϕ_{fuel} is equal to 4.0. The introduction of a diaphragm inside the injection pipe enables to deviate some of the air flow passing through the main injector by keeping constant the kerosene flow rate (the combustion chamber power is then maintained). In this configuration, the fuel stream equivalence ratio passing through the injector is increased to 6.7. Experiments have been conducted by operating all injectors under standard conditions ($\phi_{fuel} = 4.0$) except one that is modified to inject a richer fuel stream ($\phi_{fuel} = 6.7$). As shown in Fig. 3(a), the measurements by thermal painting reveal hot spots on all wall surfaces facing the injectors exit excepted for the enriched pipe.

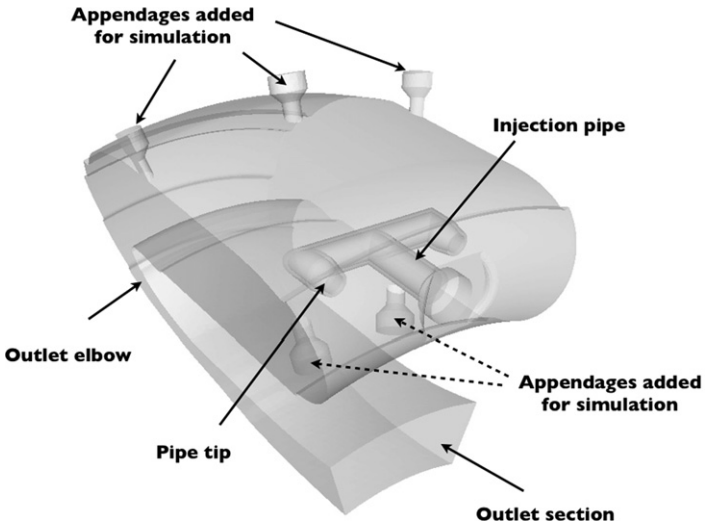

Fig. 1. Geometry of the CTA1 configuration.

Table 1
Operating conditions for cases A and B.

Combustion chamber pressure	5 bar
Fuel stream temperature	575 K
Fuel stream equivalence ratio for case A	4.0
Fuel stream equivalence ratio for case B	6.7

3.2. Numerical set-up

The simulation of the whole combustion chamber would be to expensive in term of CPU time. Therefore, CFD computations of one sector corresponding to 1/10th of the combustor rig are performed. Multi-perforations and film coolings are considered using specific boundary conditions. As the direction of the air passing through the perforated walls differs from the normal to the wall, a swirling flow is created inside the combustion chamber. Appendages visible in Fig. 1 allow to properly handle the direction and the injection of secondary air inlets. Two simulations named case A and case B are respectively conducted with a fuel stream equivalence ratio equal to 4.0 and 6.7, respectively. Operating conditions for cases A and B are summarized in Table 1. In case B, the air excess induced by the increase of fuel stream equivalence ratio has been uniformly distributed to both dilution hole and multi-perforated plate inlets. Consequently, both cases A and B operate at the same global equivalence ratio. Three visualization planes, *Downstream*, *Centerline* and *Upstream*, are defined in Fig. 2 to facilitate the 3-D flow analysis. The mesh of both cases A and B is unstructured and composed of 7,880,220 tetrahedral elements (or 1,418,848 nodes). Only the so-called primary zone in which the reaction takes place has been highly refined. Calculations are carried out with the AVBP solver [19] using the third order scheme TTGC [21]. The subgrid stress tensor is modeled by the WALE approach [22].

Two chemical lookup tables for kerosene/air combustion, representative of cases A and B operating conditions, are generated using the detailed chemical scheme proposed by Luche [23]. The mass composition of kerosene is approximated by 76.7% of $C_{10}H_{22}$, 13.2% of C_9H_{22} and 10.1% of C_9H_{18}. Unity Lewis assumption is made for this study. The progress variable Y_c is defined as $Y_c = Y_{CO} + Y_{CO_2}$ [8]. As NO_x formation is not considered, the mixture fraction z is defined from the nitrogen mass fraction $Y_z = Y_{N_2}$. This coordinate is normalized as:

$$z = \frac{Y_z - Y_z^{ox}}{Y_z^f - Y_z^{ox}} \tag{8}$$

where z varies between zero and unity. Y_z^f and Y_z^{ox} represent values of Y_z in fuel stream (here a mixture of kerosene and air characterized by an equivalence ratio ϕ_{fuel}) and oxidizer stream (here pure air). Under case A (B) operating conditions, the stoichimetric values of mixture fraction are $z_{st} = 0.3$ ($z_{st} = 0.2$) for $\phi_{fuel} = 4.0$ ($\phi_{fuel} = 6.7$). Both chemical look-up tables are filtered by a Gaussian function operator of size $\Delta = 5.4\delta_l$ where δ_l is the thermal layer thickness of the stoichiometric flame front. This choice ensures at least a computation of the filtered flame front over 4 nodes which is the minimal resolution required to avoid numerical artifact. The subgrid flame wrinkling Ξ introduced in Eqs. (2) and (7) is modeled by the formulation of Charlette et al. [24].

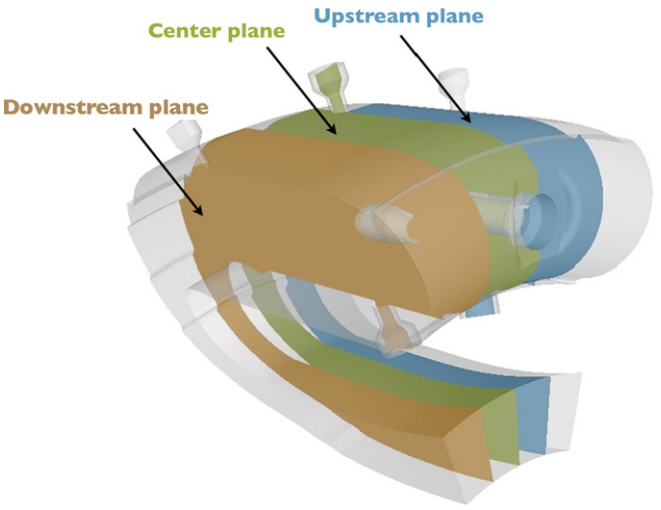

Fig. 2. Visualization planes.

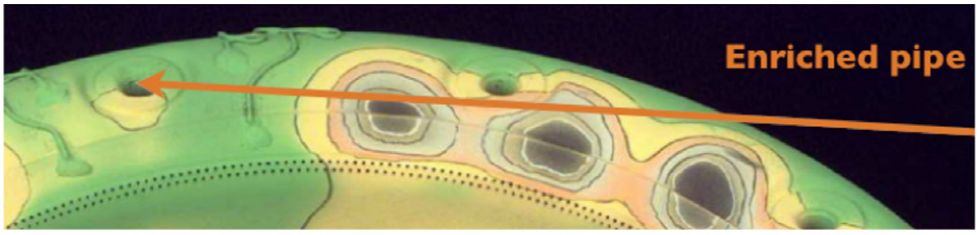

(a) Thermal painting

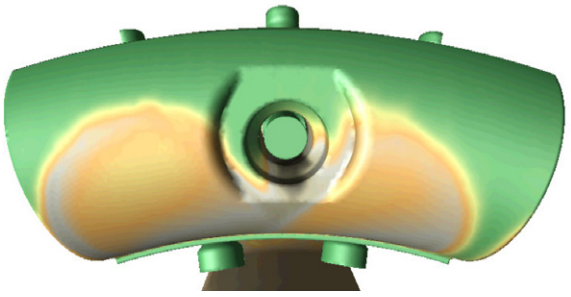

(b) F-TACLES simulation of case A

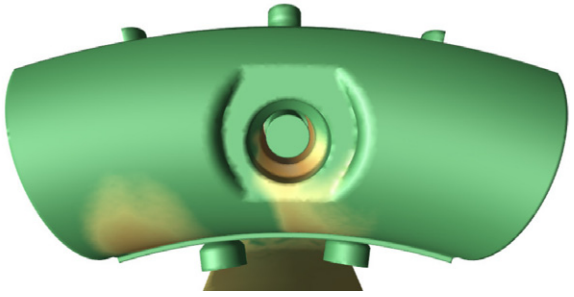

(c) F-TACLES simulation of case B

Fig. 3. Mean temperature fields from measurement and simulations on the wall surface facing the injector exit. The black and green colors respectively corresponds to high and low temperatures. (For interpretation of the references to color in this figure, the reader is referred to the web version of this article.)

3.3. Results analysis

Cases A and B are both computed over the same time period of 31 ms to obtain comparable statistics. A comparison between measured and computed data is proposed in Fig. 3 where the average temperature fields on the wall surface facing the injector exit are shown. The same color palettes are used for both numerical and experimental results. Accordingly to the experiment, the hot regions visible in the nominal configuration (case A) disappear when the fuel stream equivalence ratio is increased (case B). The apparition of these hot spots is actually due to the mixing between fuel and air. Indeed, Fig. 4 shows the prediction of mixture fraction field for both cases A and B. In the nominal configuration, stoichiometric conditions ($z_{st} = 0.3$) are encountered on the wall surfaces, leading to temperature peaks. At the opposite, the mixture fraction remains bellow the stoichiometric conditions for case B and therefore the temperature field remains close to the air stream temperature. 2-D visualization of mixture fraction fields in *Upstream* (Fig. 5) and *Downstream* (Fig. 6) planes, shows that unlike to case A, the fuel jet does not impact the wall in case B: the stoichiometric line is displaced and therefore the combustion occurs away from the wall. The mixing distribution along the *Centerline* plane is also strongly

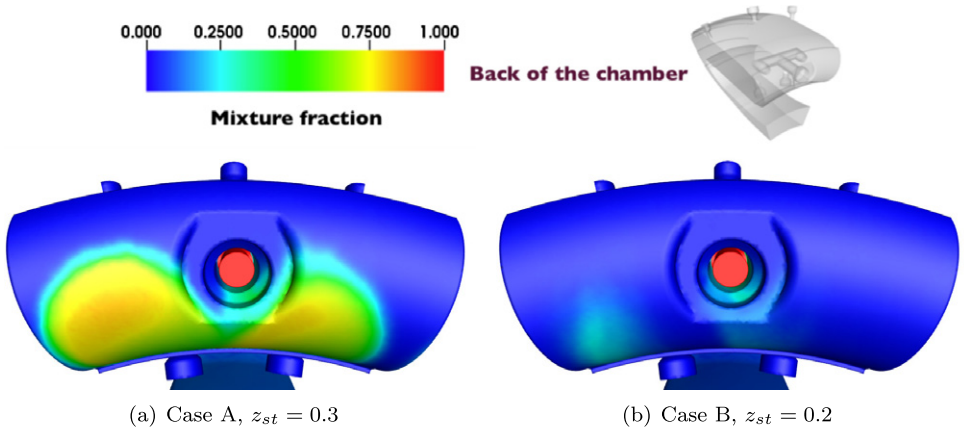

(a) Case A, $z_{st} = 0.3$ (b) Case B, $z_{st} = 0.2$

Fig. 4. Computed mean mixture fraction fields on the wall surface facing the injector exit.

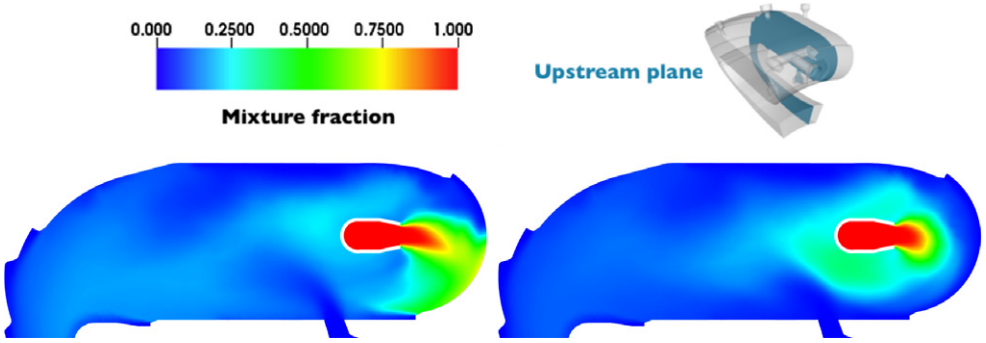

(a) Case A (b) Case B

Fig. 5. Mean mixture fraction fields on the upstream plane.

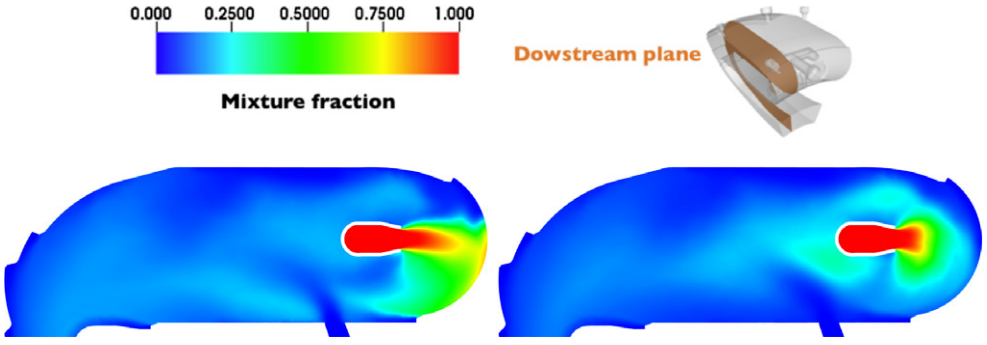

(a) Case A (b) Case B

Fig. 6. Mean mixture fraction fields on the downstream plane.

affected as illustrated in Fig. 7. Figs. 8, 9 and 10, illustrate that the change of the jet structure also affects the temperature field.

In case B, because of the reduced air flow rate passing through the injector, the jet fuel momentum is decreased by 37%. The cooling efficiency of the multi-perforated wall is increased and prevent the fuel jet from impacting the wall combustor. This phenomenon is shown in Fig. 11 where norm of velocity is shown. The hot regions evidenced from the thermal painting measurement are then due to the importance of the fuel jet momentum that impact the wall surface. For higher values of fuel stream equivalence ratio, the jet penetration is reduced by the air passing through the perforated wall.

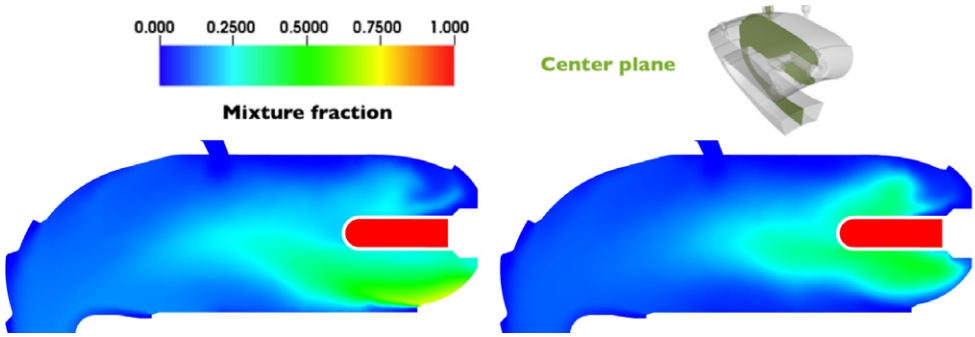

(a) Case A (b) Case B

Fig. 7. Mean mixture fraction fields on the centerline plane.

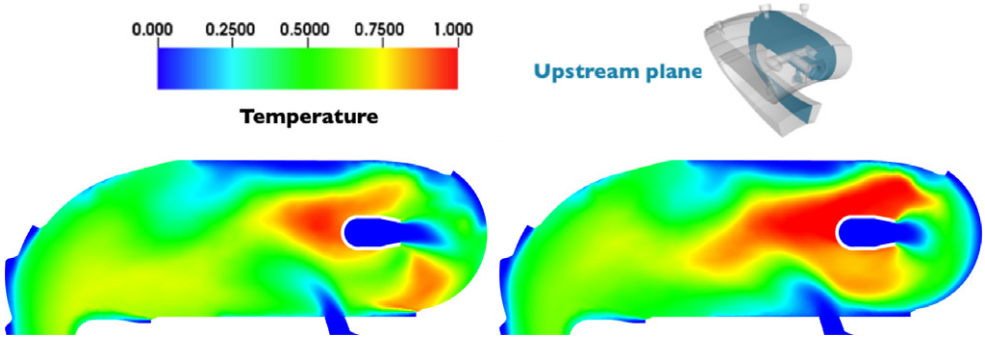

(a) Case A (b) Case B

Fig. 8. Normalized mean temperature fields on the upstream plane.

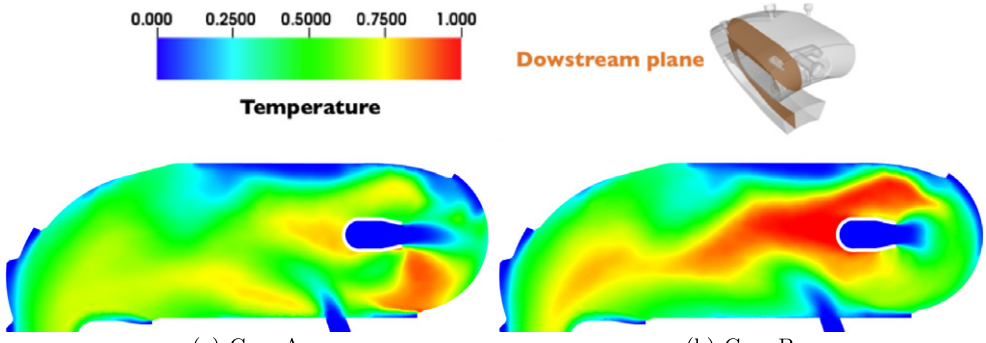

(a) Case A (b) Case B

Fig. 9. Normalized mean temperature fields on the downstream plane.

4. Conclusion

A recently developed LES turbulent combustion model that accounts for detailed chemistry effect has been used to perform the numerical investigation of a realistic helicopter combustion chamber. Two simulations have been performed that differ by the fuel stream injection conditions, i.e. both equivalence ratio and the velocity. The numerical solutions present conclusions similar to the experimental measurements achieved by thermal painting. The analysis of the LES mean flow field shows that the origin of the hot regions observed at the wall combustor surface are in fact due to the fuel jet stream momentum ratio. When increasing the fuel equivalence ratio, the fuel stream momentum decreases and therefore the wall temperature decreases.

Acknowledgements

We are grateful to Dr. Thomas Lederlin and Dr. Claude Bérat for providing us the burner geometry and the experimental data. This work was supported by the ANR-07-CIS7-008-04 Grant of the French Ministry of Research and accessed to the

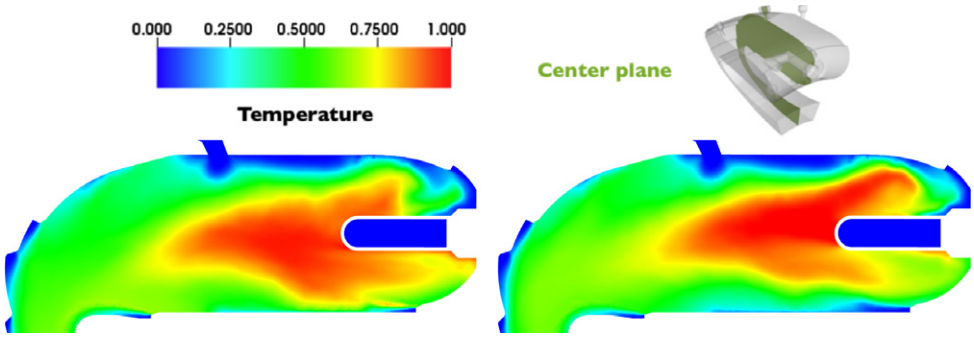

Fig. 10. Normalized mean temperature fields on the center plane.

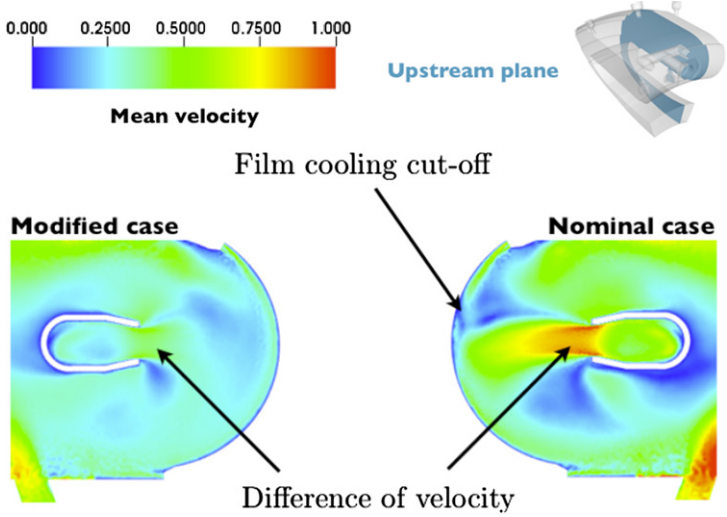

Fig. 11. Norm of mean velocity in the *Upstream* plane. Right: case A. Left: case B.

high performance computing resources of IDRIS and CINES under the allocation 2009-i2009020164 made by GENCI (Grand Equipement National de Calcul Intensif).

References

[1] A. Unal, Y. Hu, M. Chang, M.T. Odman, A. Russell, Airport-related emissions and impacts on air quality: Application to the Atlanta International Airport, Atmos. Environ. 39 (3) (2005) 5787–5798.
[2] U. Stopper, M. Aigner, H. Ax, W. Meier, R. Sadanandan, M. Stöhr, A. Bonaldo, PIV, 2D-LIF and 1D-raman measurements of flow field, composition and temperature in premixed gas turbine flames, Exp. Therm. Fluid Sci. 34 (3) (2010) 396–403.
[3] M. Boileau, G. Staffelbach, B. Cuenot, T. Poinsot, C. Berat, LES of an ignition sequence in a gas turbine engine, Combust. Flame 154 (1–2) (2008) 2–22.
[4] M. Ihme, H. Pitsch, Modeling of radiation and nitric oxide formation in turbulent nonpremixed flames using a flamelet/progress variable formulation, Phys. Fluids 20 (5) (2008) 055110, http://dx.doi.org/10.1063/1.2911047, http://link.aip.org/link/?PHF/20/055110/1.
[5] W.-W. Kim, S. Menon, H.C. Mongia, Large-eddy simulation of a gas turbine combustor flow, Combust. Sci. Technol. 143 (1999) 25–62.
[6] U. Maas, S. Pope, Simplifying chemical kinetics: Intrinsic low-dimensional manifolds in composition space, Combust. Flame 88 (1992) 239–264.
[7] O. Gicquel, N. Darabiha, D. Thévenin, Laminar premixed hydrogen/air counterflow flame simulations using flame prolongation of ILDM with differential diffusion, Proc. Combust. Inst. 28 (2000) 1901–1908.
[8] B. Fiorina, R. Baron, O. Gicquel, D. Thévenin, S. Carpentier, N. Darabiha, Modelling non-adiabatic partially-premixed flames using flame prolongation of ILDM, Combust. Theory Model. 7 (2003) 449–470.
[9] J. van Oijen, L.P.H. de Goey, A numerical study of confined triple flames using a flamelet-generated manifold, Combust. Theory Model. 8 (2004) 141–163.
[10] P. Domingo, L. Vervisch, D. Veynante, Large-eddy simulation of a lifted methane jet flame in a vitiated coflow, Combust. Flame 152 (3) (2008) 415–432.
[11] B. Fiorina, R. Vicquelin, P. Auzillon, N. Darabiha, O. Gicquel, D. Veynante, A filtered tabulated chemistry model for LES of premixed combustion, Combust. Flame 157 (2010) 465–475.
[12] G. Kuenne, A. Ketelheun, J. Janicka, LES modeling of premixed combustion using a thickened flame approach coupled with FGM tabulated chemistry, Combust. Flame 158 (9) (2011) 1750–1767.
[13] P. Auzillon, O. Gicquel, N. Darabiha, D. Veynante, B. Fiorina, A filtered tabulated chemistry model for LES of stratified flames, Combust. Flame 159 (8) (2012) 2704–2717.
[14] P. Auzillon, B. Fiorina, R. Vicquelin, N. Darabiha, O. Gicquel, D. Veynante, Modeling chemical flame structure and combustion dynamics in LES, Proc. Combust. Inst. 33 (1) (2011) 1331–1338.

[15] B. Fiorina, O. Gicquel, L. Vervisch, S. Carpentier, N. Darabiha, Approximating the chemical structure of partially-premixed and diffusion counterflow flames using FPI flamelet tabulation, Combust. Flame 140 (3) (2005) 147–160.
[16] CRC, Handbook of aviation fuel properties, Tech. Rep. 635, CRC, 3650 MANSELL ROAD SUITE 140 ALPHARETTA, GA 30022, 2004.
[17] Y. Mizobuchi, S. Tachibana, J. Shinjo, S. Ogawa, T. Takeno, A numerical analysis on structure of turbulent hydrogen jet lifted flame, in: The Proceedings of the Twenty-Ninth Symposium (Int.) on Combustion, The Combustion Institute, Pittsburgh, 2002, pp. 2009–2015.
[18] T. Poinsot, D. Veynante, Theoretical and Numerical Combustion, R. T. Edwards, Inc., 2005.
[19] http://www.cerfacs.fr/cfd/avbpcode.php, http://www.cerfacs.fr/cfd/cfdpublications.htm.
[20] R. Vicquelin, B. Fiorina, S. Payet, N. Darabiha, O. Gicquel, Coupling tabulated chemistry with compressible CFD solvers, Proc. Combust. Inst. 33 (1) (2011) 1481–1488.
[21] O. Colin, M. Rudgyard, Development of high-order Taylor–Galerkin schemes for unsteady calculations, J. Comput. Phys. 162 (2) (2000) 338–371.
[22] F. Ducros, F. Nicoud, T. Poinsot, Wall-adapting local eddy-viscosity models for simulations in complex geometries, in: E.B.M.J. (Ed.), ICFD, 1998, pp. 293–300.
[23] J. Luche, Elaboration of reduced kinetic models of combustion. Application to a kerosene mechanism, Ph.D. thesis.
[24] F. Charlette, C. Meneveau, D. Veynante, A power-law flame wrinkling model for LES of premixed turbulent combustion, Part I: non-dynamic formulation, Combust. Flame 131 (1/2) (2002) 159–180.